Interface modulated currents in periodically proton exchanged Mg doped lithium niobate

Sabine M. Neumayer, Michele Manzo, Andrei L. Kholkin, Katia Gallo', and Brian J. Rodriguez'

Articles you may be interested in

Interface modulated currents in periodically proton exchanged Mg doped lithium niobate

Sabine M. Neumayer,[1,2] Michele Manzo,[3] Andrei L. Kholkin,[4] Katia Gallo,[3,a)] and Brian J. Rodriguez[1,2,a)]

[1]*School of Physics, University College Dublin, Belfield, Dublin 4, Ireland*
[2]*Conway Institute of Biomolecular and Biomedical Research, University College Dublin, Belfield, Dublin 4, Ireland*
[3]*Department of Applied Physics, KTH Royal Institute of Technology, Roslagstullbacken 21, 10691 Stockholm, Sweden*
[4]*Department of Physics and CICECO Aveiro Institute of Materials, 3810 193 Aveiro, Portugal and Institute of Natural Sciences, Ural Federal University, 620000 Ekaterinburg, Russia*

Conductivity in Mg doped lithium niobate (Mg:LN) plays a key role in the reduction of photorefraction and is therefore widely exploited in optical devices. However, charge transport through Mg:LN and across interfaces such as electrodes also yields potential electronic applications in devices with switchable conductivity states. Furthermore, the introduction of proton exchanged (PE) phases in Mg:LN enhances ionic conductivity, thus providing tailorability of conduction mechanisms and functionality dependent on sample composition. To facilitate the construction and design of such multifunctional electronic devices based on periodically PE Mg:LN or similar ferroelectric semiconductors, fundamental understanding of charge transport in these materials, as well as the impact of internal and external interfaces, is essential. In order to gain insight into polarization and interface dependent conductivity due to band bending, UV illumination, and chemical reactivity, wedge shaped samples consisting of polar oriented Mg:LN and PE phases were investigated using conductive atomic force microscopy. In Mg:LN, three conductivity states (on/off/transient) were observed under UV illumination, controllable by the polarity of the sample and the externally applied electric field. Measurements of currents originating from electrochemical reactions at the metal electrode PE phase interfaces demonstrate a memresistive and rectifying capability of the PE phase. Furthermore, internal interfaces such as domain walls and Mg:LN PE phase boundaries were found to play a major role in the accumulation of charge carriers due to polarization gradients, which can lead to increased currents. The insight gained from these findings yield the potential for multifunctional applications such as switchable UV sensitive micro- and nanoelectronic devices and bistable memristors. © 2016 AIP Publishing LLC. [http://dx.doi.org/10.1063/1.4943934]

I. INTRODUCTION

Highly magnesium doped lithium niobate (Mg:LN) is widely used for applications in optics such as quasi phase matched devices and waveguides.[1–3] One of the main advantages of Mg:LN over undoped LN is the high resistance to photorefraction, which describes an unintended change in the refractive index due to photoinduced space charge fields that is counteracted by the high bulk photoconductivity of Mg:LN.[4,5] Due to the key role of bulk charge transport for optical applications, corresponding studies were mainly carried out using optical methods through which the majority carriers within highly doped bulk Mg:LN were found to be holes.[6] However, the electronic functionality of a material not only depends on intrinsic properties but often originates at internal and external interfaces and can be tailored through their design.[7–9] Nevertheless, little is known about charge transport through Mg:LN and its technologically relevant

structurally modified proton exchanged (PE) phase under the influence of such interfaces. Reports of high conductivity states in macroscopic poling experiments[3,10] that involve sample electrode interfaces and externally applied electric fields have attracted attention, since these findings demonstrate potential application of Mg:LN as ferroelectric semiconductor devices. Further microscopic studies of the multifunctional interplay between switched polarization and conductivity that allow for bistable resistance states upon external application of strong electric field pulses were presented in a previous work and related to sample and voltage polarity.[11] In order to further elucidate charge transport through Mg:LN and to explore paths to novel applications, conductivity and photoconductivity were studied at constant low voltages (up to ±10 V) using conductive atomic force microscopy (cAFM) on two wedge shaped 5 mol. % MgO doped LN samples of +z and −z polarization that were periodically PE. The wedge shape geometry provides access to cross sections of the PE channels while maintaining the polar axis in the vertical direction (Figure 1), whereas the introduction of PE areas containing mobile H$^+$ allows the sample

a)Authors to whom correspondence should be addressed. Electronic addresses: brian.rodriguez@ucd.ie and gallo@kth.se
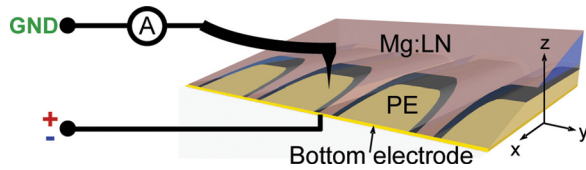
FIG. 1. Scheme of wedge shaped sample and experimental setup for current measurements.

composition dependent charge transport mechanism to be identified and the impact of charge gradients at the PE Mg:LN boundary to be studied. Other internal interfaces that have attracted high scientific interest are domain walls as they have shown abnormalities in charge transport in the absence of external electric fields in photodeposition experiments[12–15] as well as in cAFM measurements[16] under UV illumination. In the latter study, photocurrents measured at domain walls in Mg:LN and LN were associated with the inclination of domain walls and charge injection from the bottom electrode. Considering the potential that functional electronic transport at domain walls opens up for nanoscale electronic devices and sensors,[9,17–20] further studies of charge transport at these interfaces are desirable to aid practical implementation. Here, the photoconductivity of the surrounding Mg:LN and field gradients are taken into account while the sample geometry also allows to investigate non-through domains where charge injection from the bottom electrode is not permitted. The findings derived from the presented studies highlight the functional versatility of periodically PE Mg:LN, which provides tailorability of charge transport mechanisms (ionic vs. p-type photoconductivity) as well as switchable resistance states also at low voltages, which can be controlled by the orientation of the externally applied field, sample composition, and polarization, as well as UV illumination.

II. MATERIALS AND METHODS

0.5 mm-thick z-cut 5 mol. % MgO doped congruent LN samples (Roditi, Ltd.) were proton exchanged along the crystallographic x-axis by selective exposure of +z and z surfaces to benzoic acid at 230 °C for 48 h, as described elsewhere.[11,21–23] The samples were chemo-mechanically polished into a wedge shape using an alkaline sub-micron colloidal silica solution (SF1 Polishing Solution, Logitech) at an angle of ≈14°. After cleaning with organic solvents, conductive colloidal silver paint (16032, PELCO) was used to connect the sample to a gold-coated steel disc (16219-G, PELCO). For high current measurements, a ≈100 nm gold layer was deposited on the backside of the sample through thermal evaporation in vacuum and connected via colloidal silver to a conductive copper circuit board.

Contact mode AFM (MFP-3D, Asylum Research) was used to image topography. The piezoresponse from sample areas of varying compositions was measured with a piezoresponse force microscopy (PFM) where an AC voltage (5 V, 20 kHz) applied to the tip causes deformation of the surface due to the converse piezoelectric effect, allowing variations in piezoresponse to be mapped.[24,25] The resulting cantilever

movement was detected and demodulated into PFM amplitude and phase signals using an external lock-in amplifier (HF2LI, Zurich Instruments).

Currents at high voltages (tens of V) were measured with an external current amplifier (Femto DLPCA-200), while low voltage (up to ±10 V) measurements under UV were performed with a cantilever holder that includes a transimpedance amplifier (Orca sensitivity 2 nA/V, Asylum Research). In both configurations, the voltage was applied to the bottom electrode, and the tip was set to ground (GND). In order to rule out loss of conductivity due to wearing of a conductive tip coating, solid platinum probes (RMN-25PT300B, Bruker) with a nominal force constant of 18 N/m and free resonance of 20 kHz were used for all measurements.

For UV illumination, light from a deuterium UV source ($\lambda = 215$-400 nm) (D-2000S, Oceanoptics) was coupled into a fiber (QP600 2-SR, Oceanoptics), illuminating the sample from a distance around 5 mm with a power density of ≈7.6 mW/cm^2 based on the typical output power according to the manufacturer and an estimated illuminated circular surface area of 3 mm in diameter. The corresponding energy of 3.10 5.77 eV partially exceeds the bandgaps of Mg:LN (≈3.98 eV) and PE (≈3.63 eV) as obtained from continuous absorption measurements in the range of 250 450 nm on equivalent substrates with a standard spectrometer (not shown).

III. RESULTS AND DISCUSSION

The AFM topography images of the −z and +z surfaces show a difference in topography between the PE area and Mg:LN that is more pronounced at the −z surface as a result of selective etching during the chemo-mechanical polishing step (Figures 2(a), 2(b), 2(e), and 2(f)). The sample thickness is 2.5 to 6 μm from the bottom to the top of the images. PFM amplitude (Figures 2(c) and 2(d)) homogeneously decreases in the whole PE area for both polarizations, consistent with a reduction in polarization in the PE region.[26]

Subsequently recorded current measurements at ±10 V show contrast within the same PE area (Figure 3) in agreement with prior reports on undoped PE LN.[27] The PE regions consist of different phases that can be distinguished by the extent of proton exchange. The infrared spectroscopy measurements on a sample with PE areas obtained with similar process parameters (not shown) reveal absorption around 3500 cm^{-1} and around 3240 cm^{-1}. The former band is characteristic for interstitial protons whereas the lower wavenumber band represents substitutional protons.[28] With that background in mind, the contrast within the PE area shown in Figure 3 can be related to the existence of two different phases with differing proton content. From the higher currents in inner PE areas, the presence of mobile interstitial H$^+$ ions that move according to the applied electric field can be inferred. The outer PE areas show the same current behavior as Mg:LN, suggesting the absence of interstitial protons and only incorporation of H$^+$ ions that substitute for Li$^+$ ions. Dependent on the direction of the applied electric field during cAFM, the positively charged protons in PE areas move towards (for negative voltage) or away (for positive voltage) from the bottom electrode causing a small current, $I = \frac{\partial Q}{\partial t}$,
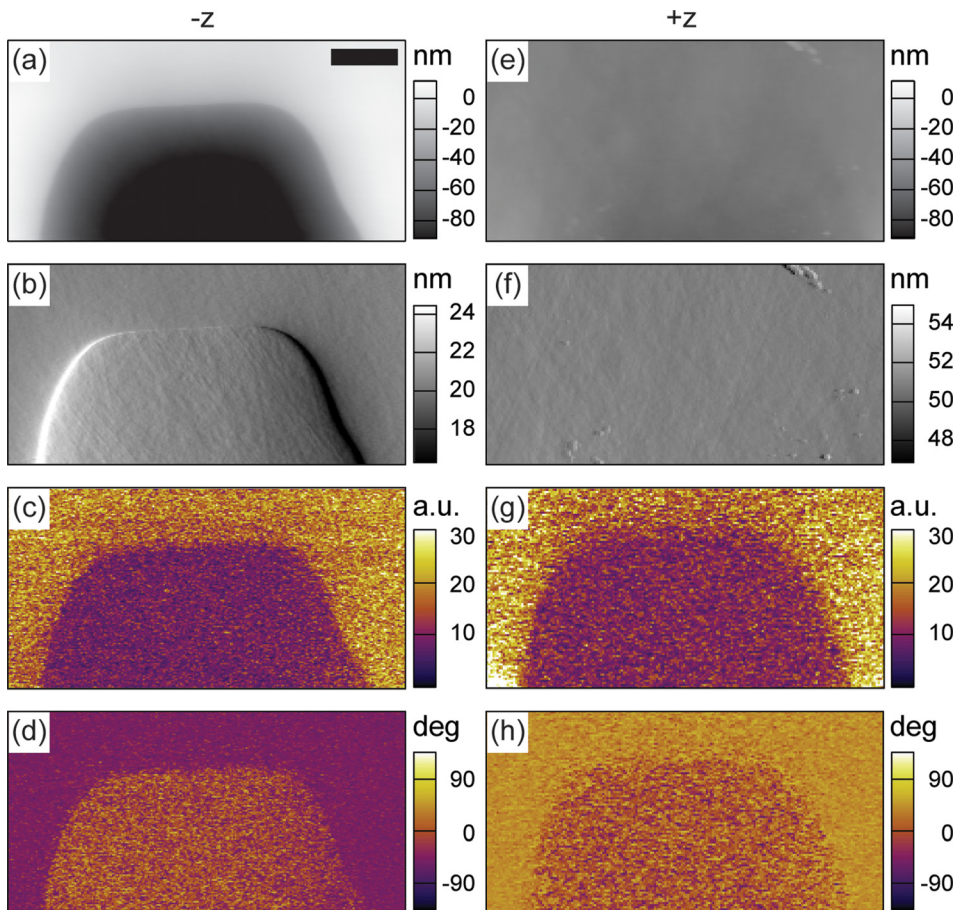
FIG. 2. AFM height (a) and (e), deflection (b) and (f), and PFM amplitude (c) and (g) and phase (d) and (h) images. The left column shows z (a) (d), while the right column shows the +z sample (e) (h) (scale bar 5 μm).

when the tip scans across areas with different capacitive properties and surface charge. The low magnitude of these currents and symmetry for positive and negative applied voltages support the attribution to a capacitive origin due to ionic charge movement. Furthermore, an increase in current with scan velocity was observed (not shown) as the tip scans horizontally across areas with different surface potential. This rate dependency is in accordance with the aforementioned equation since the detected change in charge at the sample surface increases the faster the tip moves. The polar orientation of the Mg:LN substrate does not appear to influence the polarity of the measured capacitive currents, as results obtained in Figure 3 are qualitatively the same for −z

and +z and only depend on the direction of the externally applied electric field, which is consistent with the strongly reduced polarization in PE areas.[26] However, quantitative differences can be ascribed to differences in protonation and tip-sample contact.

In current measurements under UV light, electronic conductivity through the entire circuit (voltage supply bottom electrode sample tip current amplifier GND) was observed for negative voltages in Mg:LN and confirmed by a complementary experimental setup where the current was measured with the current amplifier at the bottom electrode (not shown). However, in the PE areas, the photoinduced current flow was inhibited, and only capacitive currents due to ion
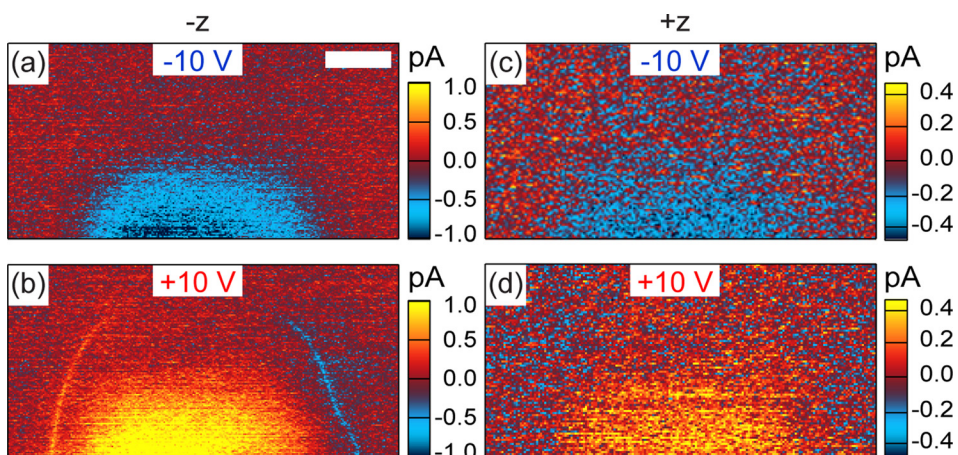

FIG. 3. Current images at (a) and (c) 10 V and (b) and (d) +10 V of the (a) and (b) z and (c) and (d) +z sample (instrumental offset subtracted; scale bar 5 μm).
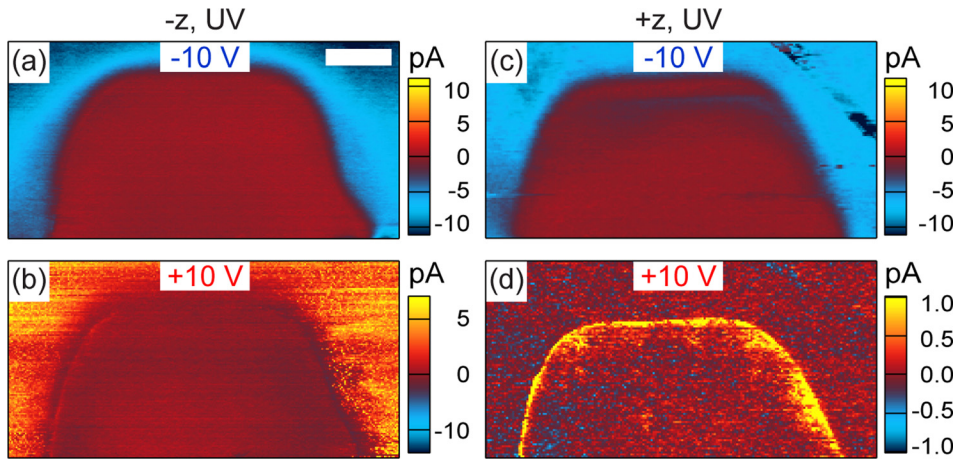
FIG. 4. Current images under UV illumination with (a) and (c) −10 V and (b) and (d) +10 V applied to the bottom electrode (instrumental offset subtracted). The left column (a) and (b) shows the −z sample; (c) and (d) right column: +z (scale bar 5 μm).

movement were observed (Figures 4(b) and 4(d)). Despite having a smaller bandgap than Mg:LN, the lower photoconductivity of the PE regions might be explained by a counteracting high recombination rate as a result of the reduced polarization.

The measured currents depend not only on the photoconductivity of a certain area but also on the metal–semiconductor interfaces at the tip and the bottom electrodes. Under application of −10 V to the bottom electrode, high negative currents were measured in Mg:LN areas (Figures 4(a) and 4(c)). When +10 V was applied, positive currents were only observed on the −z Mg:LN surfaces (Figure 4(b)) and at the boundary between the PE and Mg:LN areas (Figure 4(c)). Identical metal electrodes in contact with a p-type semiconductor can be modelled as two head to head Schottky barriers exhibiting symmetric current-voltage (IV) characteristics for positive and negative DC voltage values.[29] Asymmetries can arise due to different electrode areas, shunt resistances, and pinning of the Fermi energy by surface states. However, the depicted rectifying behavior in Figure 5 suggests that one electrode forms a Schottky contact whereas the other contact is Ohmic,[30] similar to reports on lead titanate[31] and other perovskite compounds.[32] The Ohmic behavior might be caused by flat band conditions or thermionic emission caused by illumination induced heating and high energy conduction band electrons resulting from illumination with an energy up to 1.8 eV above the bandgap.[33] Ohmic contacts occur at p-type semiconductor interfaces when the work function of
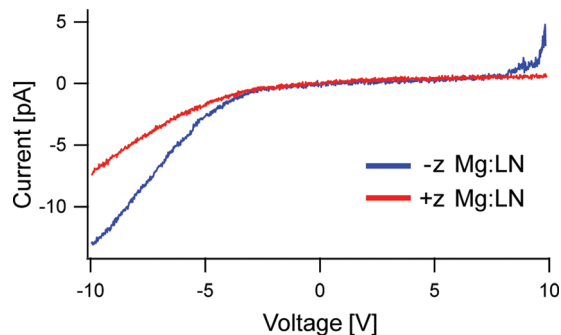
the metal is higher than that of the semiconductor $\Phi_M > \Phi_S$. As the work function of the platinum tip ($\Phi_{Pt} \approx 6.1$ eV[34]) is greater than for either silver ($\Phi_{Ag} \approx 4.2$ eV[35]) or gold ($\Phi_{Au} \approx 5.3$ eV[36]) at the bottom electrode, the Ohmic contact is assigned to be at the tip sample interface. IV curves exhibited the same qualitative characteristic with colloidal silver or a gold layer as bottom electrode (not shown).

In a simple model, the aforementioned p-type conductivity and effective screening of polarization through photogenerated charge carriers lead to downwards band bending at the sample bottom electrode interfaces for both Mg:LN polar orientations. The resulting p-type Schottky contact is conducting if a negative voltage is applied at the bottom electrode and together with the Ohmic contact at the tip, current flow is permitted. The negligible influence of the polarization direction might be attributed to effective screening by the photogenerated charge carriers and electron flow. In contrast, a positive voltage at the bottom electrode leads to a blocking interface and a continuous current flow is impeded. Furthermore, holes migrate towards the surface on the −z sample, as the depolarization and externally applied field are both pointing in the same direction. This high positive charge carrier density appears to lead to local charge injection from the tip into the sample due to a thin depletion layer.[33] However, continuous electron flow is impeded, likely due to neutralization of the positive surface charge by the injected electrons. Because of their origin, these currents occur in an irregular fashion and appear in cAFM images as short transient currents rather than a constant current value (Figure 4(b)). In the PE areas, only the low capacitive currents described previously were observed, which is ascribed to the strongly reduced polarization and low photoconductivity in that phase. On the +z sample, photocurrents originating from charge accumulation were measured at the boundary between the PE area and Mg:LN for positive voltage (Figure 4(d)). Under these conditions, holes appear to accumulate at the PE Mg:LN interface guided by electric fields across that boundary due to the spatial gradient of polarization charge,[37] facilitating spatially confined electron injection. The polarization dependent direction of the lateral electric field between the Mg:LN and PE areas can also be observed in the distribution of transient currents that are

FIG. 5. IV curves measured on Mg:LN areas of the −z and +z samples (sweep rate 4 V/s; instrumental offset subtracted).

mediated by the accumulation of positive charge carriers at these boundaries (Figures 4(b) and 4(d)). At the −z sample, holes are expected to move from the PE area towards negative polarization charge; thus, transient currents are observed only outside of the edge of a PE area. However, if the substrate is oriented in the +z direction, the positive charge carriers move in the opposite direction, towards the PE area, causing currents to be confined at the inside edge of the PE area. These lateral fields also reportedly play an important role in photodeposition experiments where photogenerated electrons can accumulate at the PE LN[37,38] or PE Mg:LN[39] interface. The previously described topographic feature at the PE Mg:LN boundary for the −z sample may obfuscate a full description of the conductivity in the vicinity of the boundary and requires further investigation. Furthermore, as the UV power density can vary between measurements due to the experimental setup, an exact quantitative comparison of currents measured on the +z and −z samples is impeded. In order to measure photocurrents of domain surfaces of opposite polarization under the same conditions and allow for direct comparison, cAFM was performed across a domain formed on the −z Mg:LN sample upon application of −100 V for 2.5 min through the conductive AFM tip. Photoinduced currents at +10 V measured at domain walls in 100 μm thick Mg:LN have been reported previously with the conclusion that conduction occurs along domain walls between the bottom electrode and the tip in an otherwise insulating material.[16] Other studies showed high conductance of charged walls adjacent to through-domains after polarization reversal with a high applied voltage.[10] Here, photocurrents across a hexagonal domain switched at an area that consists of a thin ($\approx$800 nm) Mg:LN layer that is vertically confined by a buried PE layer are investigated. Since the domain wall has no direct contact with the bottom electrode, the observed currents cannot stem from electrons injected locally by the bottom electrode. Figure 6(a) shows that at −10 V the photocurrents on both domain surfaces are of the same magnitude while enhanced currents are observed in the vicinity of the domain walls. Arbitrarily shaped domains in pure Mg:LN that are in contact with the bottom electrode exhibit the same conduction behavior (not shown), suggesting that charge injection from that electrode does not play a role in the presented work. The higher conductivity at domain walls likely stem from the local vertical and lateral electric fields arising from the polarization discontinuity in the vicinity of and across domain walls, which are expected to be inclined, thus charged, in Mg:LN.[10,16,40] The preferential surface migration of photogenerated electrons in LN at domain walls can also be observed in silver photodeposition experiments by the formation of metallic nanostructures due

to the reduction of Ag$^+$ ions along those boundaries.[12,14,15] Applying external electric fields allows for measureable current flow through electrode interfaces determined by the quantitative distribution of photogenerated charge carriers in the sample. At domain walls, charge carriers are attracted by lateral electric fields perpendicular to the domain walls. The side from which electrons and holes move towards that interface depends on the direction of the lateral field and the polarity of the charge carrier. Near domain walls, the charge carriers are also transported towards the polar surfaces by the vertical electric fields arising from the discontinuity of polarization and screening charge at the surface. When +10 V was applied (Figure 6(b)), the high positive transient currents appeared not only at the −z surface but also at the domain walls, suggesting a similar conduction mechanism as observed at the PE Mg:LN boundary (Figure 4(d)). By comparing the domain sizes in both images, the positive currents due to electrons leaving the tip (Figure 6(b)) are found to occur at the −z side of the domain wall where depolarization and screening fields are strongest towards the surface,[27,41] whereas negative currents due to electrons leaving the surface (Figure 6(a)) are not as confined and spread out into the positively poled area. These observations might be ascribed to the downward direction of the depolarization field, pushing electrons toward the surface, as well as domain wall inclination and poling induced strains.[42,43]

Electronic photoinduced currents were observed mainly on Mg:LN and not in PE areas. In the absence of UV illumination, currents originating from ionic conductance were measured in the inner PE area (expected to contain mobile interstitial H$^+$ ions) at high negative voltages (up to −90 V) applied to a gold bottom electrode (Figure 7). Due to the corresponding high electric field, H$^+$ ions move to the bottom electrode where downwards band bending allows for electron flow from the bottom electrode into the sample to reduce protons ($2H^+ + 2e^- \leftrightarrow 2H_2$). A complementary oxidation reaction is expected to take place at the tip where electrons leave the surface to close the electric circuit as mass and charge conservation must be fulfilled. The exact mechanism is currently unclear but was also measured in undoped PE LN in the same experimental setup at high positive voltages (not shown) but also at low voltages ($\leq$10 V).[27] The observed electrochemical currents exhibit a strong time, voltage, and history dependence ascribed to required activation for the electrochemical reaction. Currents were measured as a function of time while applying 5 square pulses of −90 V for 10 s with 2 s delay between pulses in the inner PE area of the −z (Figure 7(b)) and +z (Figure 7(e)) samples. From the first pulses shown in Figure 7, it is apparent that the PE phase shows memresistive behavior that manifests
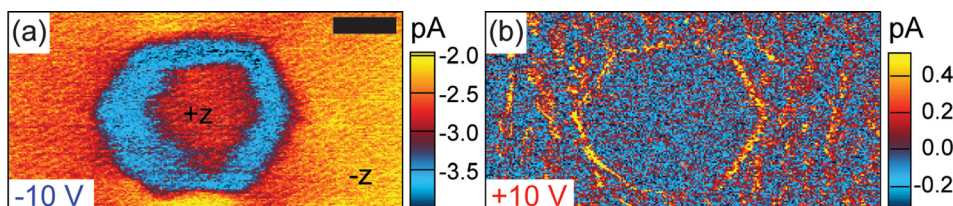

FIG. 6. Current images of domains under UV illumination with (a) −10 V and (b) +10 V applied to the bottom electrode (instrumental offset subtracted; scale bar 500 nm).
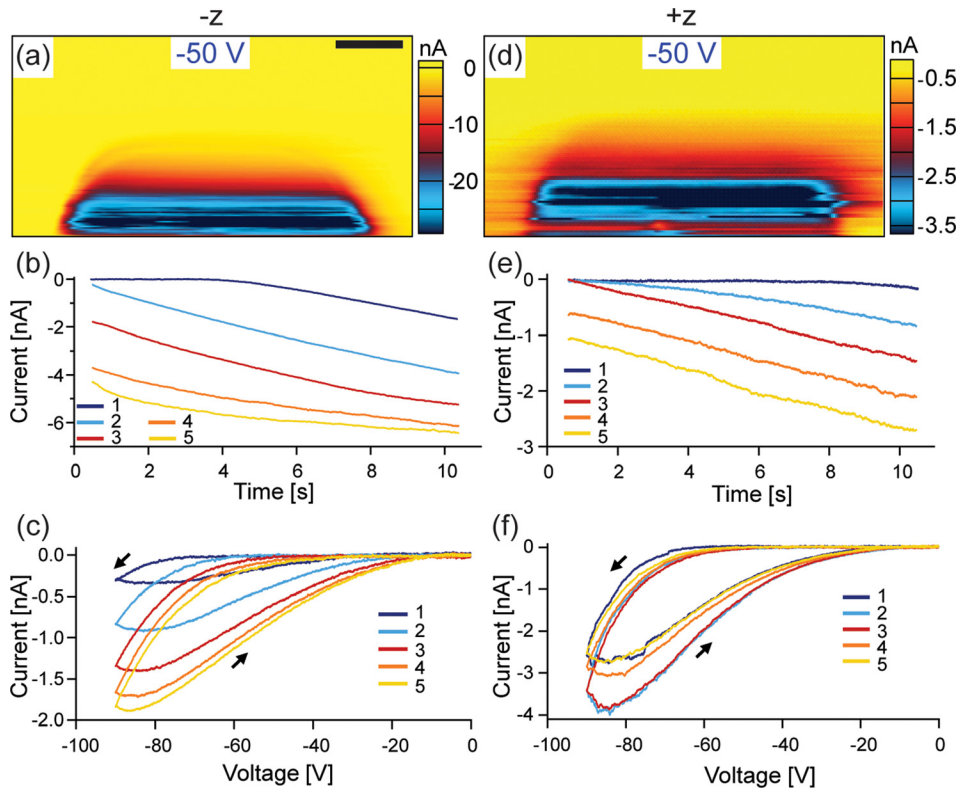
FIG. 7. Current images of (a) the −z and (d) +z PE Mg:LN samples, (scale bar 5 μm, recorded at −50 V). The current dependence on time during 5 subsequent −90 V square pulses is shown in (b) for −z and (e) for +z. IV curves for 5 subsequent triangular voltage pulses are displayed in (c) for −z and (d) for +z. Instrumental offsets subtracted for (a)–(f).

itself in the approximately linear increase in the magnitude of the currents that occurs after some activation time as well as in the appearance of higher currents with subsequent voltage pulses. Current measurements during 5 triangular voltage pulses (0 V to −90 V to 0 V within 20 s) applied subsequently in the inner PE areas on the −z (Figure 7(c)) and +z (Figure 7(f)) substrates showed hysteretic IV curves, implying a ramping direction dependence. A train of 5 square or triangular voltage pulses always lead to an increase in current with number of pulse on the −z sample. On the +z sample, this increase was not apparent in all cases (as shown in Figure 7(f)), which might be attributed to the direction of the remaining depolarization field in the PE areas that act upon the protons when the external field is removed and change band bending at the tip–sample interface, governing the accompanying oxidation reaction. Not only the applied voltage, pulse number, and voltage history is of importance, but also the amount of available H$^+$, quality of bottom electrode contact, and position of point measurements greatly influence currents and therefore limit quantitative comparison.

The same current behavior is observed when a positive voltage is applied to the tip and the bottom electrode is set to GND via an external current amplifier (not shown). Likewise, current flow was measured when high negative voltages (<-70 V) were applied to the tip, which implies that reduction in H$^+$ can also take place at the Pt tip. However, this often results in high currents ($>1\,\mu$A) and destruction of the sample, indicating the breakdown regime of those measurements. The measurement of electrochemical currents suggests that the doping induced p-type behavior that was apparent in photoconductivity measurements on Mg:LN is preserved in the PE areas.

IV. CONCLUSION

We have demonstrated that periodically PE Mg:LN yields highly functional p-type conductivity behavior that can be controlled by the polarity of the sample and applied electric field, UV illumination, as well as sample composition. Upon UV exposure, three conductivity states were observed, which are (i) ON: continuous current flow on −z and +z Mg:LN under application of negative voltages at the bottom electrode, (ii) OFF: high resistivity state on +z Mg:LN at positive voltages applied to the bottom electrode, and (iii) intermittent: intermittent current flow on −z Mg:LN upon application of positive voltages to the bottom electrode. The domain walls showed enhanced continuous and intermittent conductivity whereas the Mg:LN PE phase boundaries exhibit pronounced intermittent current flow only on the +z sample. The threefold switchability of conductivity states and tailorable internal interfaces through ferroelectric poling and introduction of PE phases yield potential applications as UV sensitive micro- and nanoelectronic devices. Without UV illumination, the movement of H$^+$ ions within the PE phase leads to capacitive currents at low voltages (up to ±10 V). However, under application of high voltages (tens of V), inner PE phases exhibit memresistive and rectifying conductivity due to electrochemical reactions at the bottom electrode–PE phase interface, which allows for practical use as solid electrolytes as well as bistable memristor devices. The insight gained into charge transport upon varying

conditions facilitates applications of periodically PE Mg:LN in multifunctional electronic devices and might also be applicable to similar semiconducting and/or ferroelectric materials.

ACKNOWLEDGMENTS

[1]Y. Chen, W. Yan, J. Guo, S. Chen, G. Zhang, and Z. Xia, Appl. Phys. Lett. **87**, 212904 (2005).

[2]K. Nakamura, J. Kurz, K. Parameswaran, and M. M. Fejer, J. Appl. Phys. **91**, 4528 (2002).

[3]K. Mizuuchi, A. Morikawa, T. Sugita, and K. Yamamoto, J. Appl. Phys. **96**, 6585 (2004).

[4]D. A. Bryan, R. Gerson, and H. E. Tomaschke, Appl. Phys. Lett. **44**, 847 (1984).

[5]K. Sweeney, L. Halliburton, D. Bryan, R. Rice, R. Gerson, and H. Tomaschke, J. Appl. Phys. **57**, 1036 (1985).

[6]H. Wang, J. Wen, J. Li, H. Wang, and J. Jing, Appl. Phys. Lett. **57**, 344 (1990).

[7]C. Sudhama, A. C. Campbell, P. D. Maniar, R. E. Jones, R. Moazzami, C. J. Mogab, and J. C. Lee, J. Appl. Phys. **75**, 1014 (1994).

[8]J. Rodriguez Contreras, H. Kohlstedt, U. Poppe, R. Waser, C. Buchal, and N. A. Pertsev, Appl. Phys. Lett. **83**, 4595 (2003).

[9]G. Catalan, J. Seidel, R. Ramesh, and J. F. Scott, Rev. Mod. Phys. **84**, 119 (2012).

[10]V. Y. Shur, I. S. Baturin, A. R. Akhmatkhanov, D. S. Chezganov, and A. A. Esin, Appl. Phys. Lett. **103**, 102905 (2013).

[11]S. M. Neumayer, E. Strelcov, M. Manzo, K. Gallo, I. I. Kravchenko, A. L. Kholkin, S. V. Kalinin, and B. J. Rodriguez, J. Appl. Phys. **118**, 244103 (2015).

[12]J. N. Hanson, B. J. Rodriguez, R. J. Nemanich, and A. Gruverman, Nanotechnology **17**, 4946 (2006).

[13]Y. Sun and R. J. Nemanich, J. Appl. Phys. **109**, 104302 (2011).

[14]Y. Sun, B. S. Eller, and R. J. Nemanich, J. Appl. Phys. **110**, 084303 (2011).

[15]N. C. Carville, S. M. Neumayer, M. Manzo, M. A. Baghban, I. N. Ivanov, K. Gallo, and B. J. Rodriguez, J. Appl. Phys. **119**, 054102 (2016).

[16]M. Schroder, A. Haußmann, A. Thiessen, E. Soergel, T. Woike, and L. M. Eng, Adv. Funct. Mater. **22**, 3936 (2012).

[17]J. Seidel, L. W. Martin, Q. He, Q. Zhan, Y. H. Chu, A. Rother, M. E. Hawkridge, P. Maksymovych, P. Yu, M. Gajek, N. Balke, S. V. Kalinin, S. Gemming, F. Wang, G. Catalan, J. F. Scott, N. A. Spaldin, J. Orenstein, and R. Ramesh, Nat. Mater. **8**, 229 (2009).

[18]J. Guyonnet, I. Gaponenko, S. Gariglio, and P. Paruch, Adv. Mater. **23**, 5377 (2011).

[19]I. Stolichnov, L. Feigl, L. J. McGilly, T. Sluka, X. K. Wei, E. Colla, A. Crassous, K. Shapovalov, P. Yudin, T. Alexander, and N. Setter, Nano Lett. **15**, 8049 (2015).

[20]L. J. McGilly, L. Feigl, T. Sluka, P. Yudin, A. K. Tagantsev, and N. Setter, Nano Lett. **16**, 68 (2016).

[21]M. Manzo, F. Laurell, V. Pasiskevicius, and K. Gallo, Appl. Phys. Lett. **98**, 122910 (2011).

[22]M. Manzo, F. Laurell, V. Pasiskevicius, and K. Gallo, Opt. Mater. Express **1**, 365 (2011).

[23]S. M. Neumayer, I. N. Ivanov, M. Manzo, A. L. Kholkin, K. Gallo, and B. J. Rodriguez, J. Appl. Phys. **118**, 224101 (2015).

[24]S. V. Kalinin, A. Rar, and S. Jesse, IEEE Trans. Ultrason. Ferroelectr. Freq. Control **53**, 2226 (2006).

[25]N. Balke, I. Bdikin, S. V. Kalinin, and A. L. Kholkin, J. Am. Ceram. Soc. **92**, 1629 (2009).

[26]M. Manzo, D. Denning, B. J. Rodriguez, and K. Gallo, J. Appl. Phys. **116**, 066815 (2014).

[27]M. Manzo, *Engineering Ferroelectric Domains and Charge Transport by Proton Exchange in Lithium Niobate* (KTH Royal Institute of Technology Stockholm, 2015).

[28]M. D. Micheli, D. Ostrowsky, J. Barety, C. Canali, A. Carnera, G. Mazzi, and M. Papuchon, J. Lightwave Technol. **4**, 743 (1986).

[29]H. Elhadidy, J. Sikula, and J. Franc, Semicond. Sci. Technol. **27**, 015006 (2012).

[30]Z. Y. Zhang, C. H. Jin, X. L. Liang, Q. Chen, and L. M. Peng, Appl. Phys. Lett. **88**, 073102 (2006).

[31]P. W. M. Blom, R. M. Wolf, J. F. M. Cillessen, and M. P. C. M. Krijn, Phys. Rev. Lett. **73**, 2107 (1994).

[32]L. Pintilie, V. Stancu, L. Trupina, and I. Pintilie, Phys. Rev. B **82**, 085319 (2010).

[33]T. V. Blank and Y. A. Goldberg, Semiconductors **41**, 1263 (2007).

[34]G. Derry and Z. Ji Zhong, Phys. Rev. B **39**, 1940 (1989).

[35]M. Chelvayohan and C. H. B. Mee, J. Phys. C: Solid State Phys. **15**, 2305 (1982).

[36]W. M. H. Sachtler, G. J. H. Dorgelo, and A. A. Holscher, Surf. Sci. **5**, 221 (1966).

[37]L. Balobaid, N. C. Carville, M. Manzo, K. Gallo, and B. J. Rodriguez, Appl. Phys. Lett. **102**, 042908 (2013).

[38]N. C. Carville, M. Manzo, S. Damm, M. Castiella, L. Collins, D. Denning, S. A. L. Weber, K. Gallo, J. H. Rice, and B. J. Rodriguez, ACS Nano **6**, 7373 (2012).

[39]L. Balobaid, N. C. Carville, M. Manzo, L. Collins, K. Gallo, and B. J. Rodriguez, Appl. Phys. Lett. **103**, 182904 (2013).

[40]E. A. Eliseev, A. N. Morozovska, G. S. Svechnikov, V. Gopalan, and V. Y. Shur, Phys. Rev. B **83**, 235313 (2011).

[41]S. Kalinin and D. Bonnell, Phys. Rev. B **63**, 125411 (2001).

[42]Z. W. Hu, P. A. Thomas, and J. Webjorn, J. Phys. D: Appl. Phys. **28**, A189 (1995).

[43]D. A. Scrymgeour and V. Gopalan, Phys. Rev. B **72**, 024103 (2005).